MCAT Institute
Annual Report
94-22

Computational Analysis of Forebody Tangential Slot Blowing on the High Alpha Research Vehicle

Ken Gee

N95-11367
Unclas
G3/02 0022235
(NASA-CR-196750) COMPUTATIONAL ANALYSIS OF FOREBODY TANGENTIAL SLOT BLOWING ON THE HIGH ALPHA RESEARCH VEHICLE Annual Report, Jan. - Jul. 1994 (MCAT Inst.) 16 p

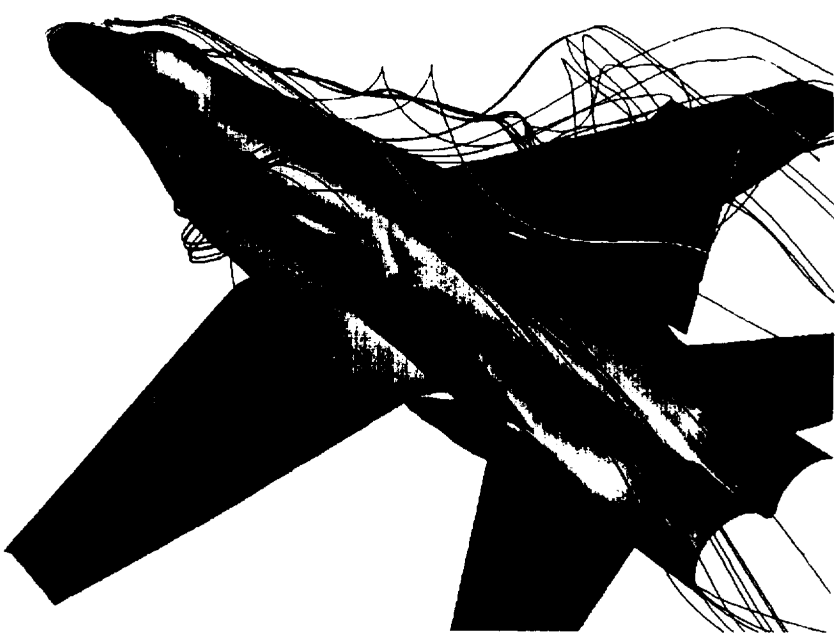

July 1994

NCC2-657

MCAT Institute
3933 Blue Gum Drive
San Jose, CA 95127

EFFECTIVENESS OF FOREBODY TANGENTIAL SLOT BLOWING IN THE TRANSONIC FLIGHT REGIME

Report of Research Conducted Under Grant NCC2-657
January - July, 1994

Ken Gee
Principle Investigator

Current and future fighter aircraft can maneuver in the high-angle-of-attack flight regime while flying at low subsonic and transonic freestream Mach numbers. However, at any flight speed, the ability of the vertical tails to generate yawing moment is limited in high-angle-of-attack flight. Thus, any system designed to provide the pilot with additional side force and yawing moment must work in both low subsonic and transonic flight. However, previous investigations of the effectiveness of forebody tangential slot blowing in generating the desired control forces and moments have been limited to the low subsonic freestream flow regime. In order to investigate the effectiveness of tangential slot blowing in transonic flight, a computational fluid dynamics analysis was carried out during the grant period.

The flexibility of CFD as an analysis tool was evident during this work since it easily allowed for results to be obtained over a wide range of freestream Mach numbers. Such data was not available form wind tunnels due to the limitations of the tunnels previously used to investigate forebody tangential slot blowing and the high cost of fabricating new models for tunnels capable of operating in the transonic speed range. Although experimental data was not available for validation of the CFD results, the CFD tools used to obtain the results have shown to be quite accurate at the lower Mach numbers. This experience indicated that the new results at the higher Mach numbers would also be reasonably accurate.

Computational solutions were obtained at three different freestream Mach numbers and at various jet mass flow ratios. All results were obtained using the isolated F/A-18 forebody grid geometry at 30.3 degrees angle of attack. One goal of the research was to determine the effect of freestream Mach number on the effectiveness of forebody tangential slot blowing in generating yawing moment. The second part of the research studied the force onset time lag associated with blowing. The time required for the yawing moment to reach a steady-state value from the onset of blowing may have an impact on the implementation of a pneumatic system on a flight vehicle.

The computational results indicated that forebody tangential slot blowing remained effective at transonic freestream Mach numbers. Significant levels of yawing moment were generated even at moderate blowing rates. At very low blowing rates, little or no yawing moment was generated. This was due to the jet not having enough energy to significantly alter the flow field in the nose region. The jet separated along with the primary vortex on the blowing side. At very high blowing rates, overblowing occurred. In this case, the jet was underexpanded as it exited the slot. The rapid expansion of the jet forced the fluid off the surface. This lead to an early separation of the jet, compared to the moderate blowing rates, and a leveling off of the yawing moment with increasing jet mass flow ratio. Overblowing can be avoided by reducing the jet mass flow rate or increasing the slot area to reduce the jet exit pressure for a given jet mass flow rate.

The second goal of the research was to determine the force onset time lag associated with forebody tangential slot blowing. Excessively long periods of time required for the yawing moment to reach a steady-state value would reduce the usefulness of the system on a flight vehicle. In order to study this problem, time-accurate solutions were obtained at one mass flow ratio and three freestream Mach numbers using the isolated forebody geometry. These results should be indicative of the lag times associated with the full aircraft geometry.

The solutions indicate that the force onset time lag for the forebody geometry was on the order of one non-dimensional time unit, based on freestream velocity and forebody length. This meant that the yawing moment reached a steady-state value in the time a particle require to travel the length of the forebody, regardless of the freestream velocity. This result compared well with the data obtained in full-scale and sub-scale wind tunnel tests. The lag time was not significant, and was on the order of the response time of the vertical tail at a lower angle of attack. A more detailed analysis of the results was presented at the 12th AIAA Applied Aerodynamics Conference. A copy of the paper is included as Appendix A.

The investigation conducted during the grant period produced useful information about the capabilities of forebody tangential slot blowing as a means of generating yawing moment on an aircraft flying at high angle of attack. The data added to the existing knowledge base which may prove useful to designers of current and future high-performance aircraft. Through the use of such innovative devices such as forebody tangential slot blowing, safer and more efficient aircraft can be developed to better serve the needs of the public.

Appendix A

AIAA-94-1831

ANALYSIS OF TANGENTIAL SLOT BLOWING ON F/A-18 ISOLATED FOREBODY

Ken Gee
MCAT Institute
Moffett Field, CA

Yehia M. Rizk and Lewis B. Schiff
NASA-Ames Research Center
Moffett Field, CA

AIAA 12th
Applied Aerodynamics Conference
June 20-23, 1994 / Colorado Springs, CO

ANALYSIS OF TANGENTIAL SLOT BLOWING ON F/A-18 ISOLATED FOREBODY

Ken Gee*
MCAT Institute
Moffett Field, CA 94035

Yehia M. Rizk† and Lewis B. Schiff‡
Ames Research Center
Moffett Field, CA 94035

Abstract

Generation of significant side forces and yawing moments on an F/A-18 fuselage through tangential slot blowing is analyzed using computational fluid dynamics. The effects of freestream Mach number, jet exit conditions, jet length, and jet location are studied. The effects of over- and under-blowing on force and moment production are analyzed. Non-time-accurate solutions are obtained to determine the steady-state side forces, yawing moments, and surface pressure distributions generated by tangential slot blowing. Time-accurate solutions are obtained to study the force onset time lag of tangential slot blowing. Comparison with available experimental data from full-scale wind tunnel and sub-scale wind tunnel tests are made. This computational analysis complements the experimental results and provides a detailed understanding of the effects of tangential slot blowing on the flow field about the isolated F/A-18 forebody. Additionally, it extends the slot-blowing database to transonic maneuvering Mach numbers.

Introduction

The use of pneumatic forebody flow control on aircraft flying at high angle of attack has been a topic of aerodynamic research over the past several years. The flow field about an aircraft at high incidence is characterized by crossflow separations of the boundary layer, which then roll up to form vortices. At high angle of attack these vortices may become asymmetric, creating a side force and yawing moment on the aircraft, which can cause an uncontrolled departure of the aircraft from its intended flight path. Furthermore, flight at high angle of attack immerses the vertical tails in the wake of the fuselage and wing, reducing the effectiveness of these control surfaces. In order to provide the necessary control power to the pilot to maintain controlled flight, new methods of generating control forces and moments must be developed.

One such method under investigation is forebody tangential slot blowing.[1,2] In this method, a thin slot is located near the tip of the nose of an aircraft from which air is ejected tangential to the nose surface (Fig. 1). The jet remains attached to the surface due to the Coanda effect and eventually separates. The jet alters the flow field about the aircraft, which in turn generates a side force and yawing moment. This side force and yawing moment may then be used by the pilot to control the aircraft at high angle of attack.

Both experimental and computational investigations have been used to analyze the effectiveness of tangential slot blowing on the F/A-18. Experiments have been conducted on sub-scale models in water tunnels[3] and wind tunnels,[4] and on a full-scale model in a wind tunnel.[5] Computational investigations have been conducted on both the isolated F/A-18 forebody[2] and on the full aircraft geometry.[6] These investigations have shown tangential slot blowing to be a viable method of generating side force and yawing moment on an aircraft flying at high angle of attack at relatively low freestream Mach numbers. To date, only low freestream Mach numbers have been investigated experimentally, due to the limitations of the facilities used. Similarly, previous computational studies have only been carried out at low freestream Mach numbers to compare with the experimental data.

However, a maneuvering fighter may attain high-angle-of-attack flight at higher Mach numbers. The capability of forebody tangential slot blowing at higher freestream Mach numbers is not well understood. To develop such an understanding, a computational investigation is presented which analyzes the efficiency of tangential slot blowing at higher freestream Mach numbers. The

---

* Research Scientist. Member, AIAA.
† Research Scientist. Associate Fellow, AIAA.
‡ Special Assistant for High Alpha Technology. Associate Fellow, AIAA.

numerical method employed has been shown to produce good results at the lower Mach numbers, when compared with available experimental data.[6] Thus, there is confidence in the ability of the numerical method to accurately predict the trends at the higher freestream Mach numbers.

Computational results are obtained for an isolated F/A-18 fuselage forebody at three freestream Mach numbers. No-blowing solutions are obtained to investigate the effects of Mach number on the baseline flow fields. The trends obtained from the no-blowing solutions are compared with available experimental data. Two different active slot configurations are investigated at each freestream Mach number. Five different mass flow ratios (MFR) are used with each slot configuration (Table 1). MFR is defined as the ratio of the jet mass flow rate to a reference mass flow rate based on freestream density and velocity and the wing surface area. The results of the analysis provides an understanding of the effect of freestream Mach number on the efficiency of tangential slot blowing.

The next section briefly describes the numerical method, turbulence model, and grid systém used in this investigation. The computational results are then presented and discussed. Conclusions are then drawn based on the analysis of the data.

Numerical Method

Since flow about a body at high angle of attack involves viscous effects and three-dimensional separated flow, the three-dimensional Navier-Stokes equations must be solved to accurately resolve the relevant flow features. Solution of the three-dimensional thin-layer Navier-Stokes equations are obtained using the F3D code, reported by Steger, Ying, and Schiff.[7] This code has been used extensively over the past several years to accurately predict the flow field about the isolated F/A-18 forebody[8] and full F/A-18 geometry[9] at high angle of attack. Since the flow fields of interest are turbulent in nature, the Baldwin-Lomax algebraic turbulence model[10] with modifications by Degani and Schiff[11] is used. A complete description of the numerical method and the code may be found in Refs. 7 and 12.

The grid system used to model the isolated F-18 forebody in the present computations, shown schematically in Fig. 2, is similar to that used by Gee et al. in Ref. 6. The grid system consists of six grids and uses the overset grid method[13] to facilitate boundary data transfer among the grids. The slot geometry is modeled in this grid system by the use of two grids in the nose of the forebody (Fig. 2). The physical slot geometry is patterned after the slot configuration used in the full-scale wind tunnel experiments[5] (Fig. 3). In the experimental setup, the slot was divided into six eight-inch segments individually connected to valves. In this way, the active slot length and location could be varied during the experiment. The jet length is varied in the computational results through the use of appropriate boundary conditions.

The jet is modeled computationally by using boundary conditions to introduce the jet exit conditions into the flow field. If the jet exit Mach number is less than sonic, the jet total pressure and total temperature are input into the flow solver. The exit pressure is obtained by extrapolating the pressure from the local external flow pressure at the jet exit and the jet exit Mach number is obtained using the isentropic relations. For sonic flow, the jet is assumed to choke at the exit and the jet exit pressure is obtained from isentropic relations using the jet total pressure and temperature inputs. In either case, in order to obtain the desired MFR value, the total pressure of the jet is increased, thereby increasing the jet density, until the desired jet mass flow rate is obtained. In addition, a no-slip boundary condition is applied at the forebody surface, freestream conditions are maintained at all inflow boundaries, and a zero-gradient extrapolation in the axial direction is used at the exit boundary.

Results and Discussion

One objective of the computational investigation is to determine the effect of freestream Mach number on the efficiency of tangential slot blowing. Therefore, computed no-blowing and blowing solutions are obtained for flow about an isolated F-18 forebody at $\alpha = 30.3°$ at three different freestream Mach numbers, $M_\infty = 0.243$, 0.400, and 0.700. The corresponding Reynolds numbers, based on the F/A-18 wing mean aerodynamic chord, are $Re_{\bar{c}} = 11.0 \times 10^6$, 18.0×10^6, and 31.4×10^6, respectively.

No-Blowing Solutions

No-blowing solutions are obtained at each freestream Mach number and serve as baseline solutions from which the blowing solutions are computed. Analysis of the no-blowing solutions also serve as a check to insure that the numerical method is accurately predicting the flow fields and the relevant trends. Although details of the flow field are similar to results presented previously,[6] the main features are briefly discussed for comparison with the blowing results.

Flow Field Characteristics

Figure 4 shows the surface flow pattern and off-surface instantaneous streamlines obtained from the solution computed at $M_\infty = 0.700$. The flow field is similar to that reported in previous work with the isolated F/A-18 forebody at a lower freestream Mach number.[6] There are a primary and secondary separation line on each side of the forebody barrel. Flow which separates from the forebody rolls up to form vortices above the forebody (Fig. 4b). Each wing leading edge extension (LEX) has a sharp leading edge and a primary crossflow separation line lies along this edge. A secondary separation line is also evident on the upper surface of each LEX (Fig. 4a). At this angle of attack, the no-blowing flow field is symmetric.

Surface Pressure Coefficient Comparison

Figure 5 shows a comparison of the computational and experimental[14] spanwise surface pressure distributions for the two higher Mach number cases at three axial locations on the LEX. Experimental data show a reduction in the suction peaks with increasing freestream Mach number.[14] This trend is also evident in the computational results. The computation obtained at $M_\infty = 0.400$ underpredicts the suction peaks on the LEX. However, the comparison of the data for $M_\infty = 0.700$ is quite good, especially at the upstream LEX stations, F.S. 253 and F.S. 296. The comparison worsens slightly at F.S. 357.

The underprediction of the LEX suction peaks at the lower Mach number may be due to the use of the isolated forebody in the computations. Previous results[8] using the isolated forebody also underpredict the surface pressure coefficient. However, addition of the wing and tail geometry produced a better comparison with flight test data.[9] By including the wing and tail, LEX vortex burst is resolved. This affects the surface pressure, especially on the last pressure station, F.S. 357, since the burst occurs in this region. The comparison at the higher freestream Mach number is better since at the higher Mach number, the influence of downstream effects on the flow at a given axial location is reduced. The overall good agreement in the trends with increasing Mach number shown in the no-blowing solutions provide confidence that the analogous trends seen in the computed blowing solutions will also be valid.

Blowing Solutions

Solutions with blowing are obtained at each freestream Mach number using two active slot configurations. One configuration consists of a 16 in. active slot beginning 11 in. aft of the nose (hereafter referred to as the 16-11 in. slot). The other slot configuration has a 24 in. slot beginning 3 in. aft of the nose (24-3 in. slot). Blowing occurs only on the port side (pilot's view) of the forebody. For each slot configuration and freestream Mach number, solutions are obtained at five mass flow ratios (MFR) ranging from 0.03 x 10^{-3} to 0.24 x 10^{-3} (Table 1). At $M_\infty = 0.243$, additional cases are computed for MFR = 0.015 x 10^{-3}. The results permit evaluation of the effect of varying Mach number, at a fixed MFR, on the efficiency of tangential slot blowing, as well as the effect of varying MFR at a fixed Mach number.

Yawing Moment Comparison

The yawing moment, C_n, obtained from blowing is plotted against MFR for both slot configurations in Fig. 6. The moment center used to compute C_n is located at the center of gravity point of the aircraft, F.S. 454 (Fig. 3). As was seen previously in sub-scale[4] and full-scale[5] wind-tunnel tests, the mass flow ratio is a good parameter for correlating the forces produced by blowing at differing flow conditions.

The computed results show that both slots configurations are capable of generating yawing moment, even at transonic maneuvering Mach numbers. For both slot configurations at $M_\infty = 0.243$ and 0.400, the yawing moment increases with increasing MFR. For the case with the 16-11 in. slot at $M_\infty = 0.700$, the yawing moment first increases, then levels off and decreases slightly as the MFR increases. A similar, but less pronounced, leveling off of C_n also occurs for the 24-3 in. slot at $M_\infty = 0.700$. However, useful yawing moments are obtained at moderate jet mass flow rates at all freestream Mach numbers (Table 1). Further analysis of the computed flow fields yields information about the flow physics associated with the behavior of the curves shown in Fig. 6.

Flow Field Analysis

At the lowest blowing rate analyzed, MFR = 0.015 x 10^{-3}, almost no yawing moment is obtained for either slot configuration. This is consistent with the sub-scale results obtained by Kramer et al.[4] At this angle of attack, no force reversal was observed in either the experimental or computational data.

The computed surface flow pattern and off-surface instantaneous streamlines, obtained from the 16-11 in slot, $M_\infty = 0.243$, MFR = 0.015 x 10^{-3} solution (Fig. 7), show the jet separating along with the blowing-side primary forebody vortex. There is no change in the position of the blowing-side primary separation line on the forebody barrel (Fig. 7a). The off-surface instantaneous streamlines (Fig. 7b) show the jet to have almost no effect on the position of either the blowing-side or non-blowing-side forebody vortex. The early separation reduces the low pressure region caused by the attached jet and reduces the interaction of the jet with the non-blowing-side forebody vortex. Both of these effects serve to reduce the amount of side force and yawing moment generated.

At MFR = 0.03 x 10^{-3}, blowing from the 16-11 in. slot generates slightly higher amounts of C_n than blowing from the 24-3 in. slot. The smaller area of the 16-11 in. slot requires a higher jet exit Mach number to obtain a given jet mass flow rate. The higher jet exit velocity increases the suction pressure generated by the attached portion of the jet. This serves to increase the yawing moment generated by blowing.

At MFR = 0.06 x 10^{-3}, the yawing moment increases slightly with increasing freestream Mach number. This is most evident in the 24-3 in. slot configuration results. Again, this is due to the differences in the jet exit Mach numbers (Table 1). As the freestream Mach number increases, the jet mass flow rate must increase to maintain a given MFR value. An increase in jet mass flow rate causes a corresponding increase in the jet exit Mach number until choked conditions are reached at the slot exit.

Once the jet is choked, the effectiveness of blowing depends upon the jet exit pressure. The ratio of the jet exit pressure, P_e, to the local static pressure, P_a, is presented in Table 1. For moderate values of this ratio, $P_e/P_a < 1.5$, C_n increases with MFR and does not depend on the freestream Mach number. This can be seen in the 24-3 in. slot results for 0.12 x 10^{-3} < MFR < 0.24 x 10^{-3}. However, for $P_e/P_a > 1.5$, the blowing effectiveness levels off. This is most evident in the 16-11 in. slot, $M_\infty = 0.700$ case. As the blowing rate, and thus the jet exit pressure, increases, the yawing moment levels off and slightly decreases for this case. This is due to the phenomenon of overblowing.

Overblowing has been observed experimentally[4] as a drop-off of yawing moment at high blowing rates. The effect of overblowing on the computed flow field is observed by plotting the velocity vectors in a crossflow plane at F.S. 75 that passes through the jet region (Fig. 8). Overblowing occurs when the jet flow is sonic and underexpanded ($P_e/P_a > 1.0$) at the slot exit. For $P_e/P_a > 1.5$, the jet rapidly expands after leaving the slot, deflecting the flow away from the fuselage surface, causing earlier crossflow separation. This action negates the Coanda effect, which causes delay of the crossflow separation. At the lower blowing rate (Fig. 8a), the jet remains attached to the surface. As the jet negotiates the curvature of the surface, the surface pressure drops, generating a low pressure region, contributing to the side force and yawing moment generated. However, in a case with overblowing, the jet does not remain attached to the surface (Fig. 8b). Rather, it separates and rides on top of a layer of fluid that is moving in the opposite direction. The separation of the jet reduces the suction generated by the jet, thereby reducing the side force and yawing moment. Side force and yawing moment are still generated due to the manipulation of the forebody vortices by the jet.

The behavior of the overblown jet is observed graphically using instantaneous streamlines to illustrate the vortices formed on the nose and the jet (Fig. 9). For the attached jet flow (Fig. 9a), blowing causes the nose vortex on the blowing side to merge with the nose vortex on the non-blowing side. The jet flow also becomes entwined in this merged nose vortex. In the overblown case (Fig. 9b), the two nose vortices do not merge, although there is still a slight interaction between the jet flow and the non-blowing-side nose vortex. This is in contrast to the very low blowing case (Fig. 7b), where no interaction between the jet and non-blowing-side forebody vortex is observed.

The behavior of the jet also has an effect on the contribution of the forebody barrel and LEX region to the yawing moment. This effect can be seen in Fig. 10, which presents the local yawing moment distribution along the forebody. Previous computational studies[6,15] indicated that there is a contribution to the side force and yawing moment from the forebody barrel aft of the slot and the LEX region. At the lowest blowing rate shown, there is almost no yawing moment evident along the entire forebody. This is due in part to the early separation of the jet. Without this flow interacting with the non-blowing-side LEX vortex, changes in the surface pressure in the LEX region is reduced. Overblowing reduces the amount of yawing moment obtained in the blowing region as well as over the remainder of the forebody. Again, this is due to the early separation of the jet and the limited interaction between the jet and the non-blowing-side nose and LEX vortices.

The phenomenon of overblowing can be avoided by limiting the jet exit pressure to 1.5 times the local static pressure in the slot region. This can be accomplished at high jet mass flow rates by increasing the area of the slot. At the high blowing rates, the larger area of the 24-3 in. slot is beneficial (Fig. 6b), since a lower jet total pressure is required to obtain a given MFR (Table 1). Overblowing starts at MFR = 0.12 x 10^{-3} for the 16-11 in. slot; for the 24-3 in. slot, the onset of overblowing does not occur until MFR = 0.24 x 10^{-3}. For both slot configurations, the computed results indicate that blowing can generate useful amounts of yawing moment at moderate blowing rates, even at transonic Mach numbers.

Force Onset Time Lag

Time-accurate solutions are obtained using the isolated F/A-18 forebody, the 16-11 in. slot configuration, and MFR = 0.06 x 10^{-3} to determine the force onset time lag associated with forebody tangential slot blowing. The forebody yawing-moment coefficients, C_n, are plotted against time, t, in Fig. 11. Blowing is activated at $t = 0.0$ in all cases. The time lag associated with charging up the plenum chamber or associated plumbing is not modeled. The yawing-moment coefficient time histories (Fig. 11) show that at $M_\infty = 0.243$, it requires about 0.15 seconds for the yawing moment to reach a maximum steady value. This value is consistent with data obtained in sub-scale[4] and full-scale[5] wind tunnel tests. As the freestream Mach number increases, the time lag decreases since it requires less time to convect disturbances downstream. In all cases, the flow field has reached its steady-state value in the time required for the freestream flow to traverse approximately three mean aerodynamic chord lengths, which corresponds to the length of the isolated forebody used in the present computations.

The time lag is also studied by examining the surface-pressure coefficient at two axial locations on the forebody barrel (Fig. 12). The two points are located on the forebody barrel on the blowing side of the body, as shown in Fig. 3. At F.S. 142, for $M_\infty = 0.243$ (Fig. 12a), the computed data shows a delay of about 0.01 seconds, followed by a ramp down of the surface pressure over a period of 0.065 seconds. This behavior is also seen in the experimental data.[5] As the freestream Mach number increases, the response time decreases. At F.S. 184 (Fig. 12b), the response times increase to 0.025 seconds and 0.075 seconds for the delay and ramp down, respectively. Again, the response time decreases with increasing Mach number. This data indicates that the time lags associated with development of yawing moments using pneumatic slot blowing for forebody flow control are not large enough to be detrimental to the usefulness of the system.

Conclusions

A computational analysis of the effect of freestream Mach number on the effectiveness of forebody tangential slot blowing was presented. The flow about an isolated F-18 forebody was computed using a thin-layer Navier-Stokes flow solver. Solutions were obtained at three different freestream Mach numbers. At each Mach number, two slot geometries and five different mass flow ratios were used. Additional solutions were obtained at the lowest freestream Mach number using an even lower mass flow ratio. Time-accurate solutions were obtained to determine the force onset time lag due to blowing.

The computational results indicated that forebody tangential slot blowing remained effective, even at transonic Mach numbers. At the very low mass flow ratios, blowing had no effect on the flow field. The jet separated along the primary separation line seen in the no-blowing solution, and did not change the position of the forebody vortices. As the mass flow ratio increased, the yawing moment generated increased. At a given mass flow ratio, the yawing moment increased with increasing freestream Mach number. This was due to the increase in the jet exit velocity. As the jet exit velocity became sonic, this effect diminished. Further increases in the mass flow ratio lead to overblowing. This was especially evident at the highest freestream Mach number and highest MFR value analyzed. Overblowing was caused by the jet being underexpanded as it left the slot. The rapid expansion of the jet caused the jet to separate from the surface. This early separation reduced the effectiveness of the pneumatic system. Unlike the low blowing rate cases, the overblown jet still had an effect on the position of the vortices and generated a significant yawing moment. Overblowing was avoided by limiting the jet exit pressure ratio. For high jet mass flow rates, this was achieved by increasing the slot area. The results showed that tangential slot blowing remained effective at transonic Mach numbers.

Time-accurate solutions were obtained using one of the slot configurations, one mass flow ratio, and all three freestream Mach numbers. The yawing moment time history and the surface pressure coefficient time history at two points on the forebody barrel were recorded for each case. The yawing moment history indicated that a steady-state value was reached in the time required for a particle in the flow field to travel approximately three mean aerodynamic chord lengths. The surface pressure coefficient indicated a small delay followed by a ramp down in pressure as the jet was convected downstream. These time lags were of the same order as those measured in full-scale and sub-scale wind tunnel tests. The results indicated that the time lags did not present an obstacle to implementation of forebody tangential slot blowing on an aircraft.

References

1. Ng, T. T. and Malcolm, G. N., "Aerodynamic Control Using Forebody Blowing and Suction," AIAA Paper 91-0619, January, 1991.

2. Gee, K., Tavella, D., and Schiff, L. B., "Computational Investigation of a Pneumatic Forebody Flow Control Concept," *Journal of Aircraft*, Vol. 30, No. 3, 1993, pp. 326-333.

3. Ng, T. T., Suarez, C. J., and Malcolm, G. N., "Forebody Vortex Control Using Slot Blowing," AIAA Paper 91-3254-CP, September, 1991.

4. Kramer, B., Suarez, C., and Malcolm, G., "Forebody Vortex Control with Jet and Slot Blowing on an F/A-18," AIAA Paper 93-3449, August, 1993.

5. Lanser, W. R., Meyn, L. A., and James, K. D.., "Forebody Flow Control on a Full-Scale F/A-18 Aircraft," AIAA Paper 92-2674, June, 1992.

6. Gee, K., Rizk, Y. M., Murman, S. M., Lanser, W. R., Meyn, L. A., and Schiff, L. B., "Analysis of a Pneumatic Forebody Flow Control Concept About a Full Aircraft Geometry," AIAA Paper 92-2678, June, 1992.

7. Steger, J. L., Ying, S. X., and Schiff, L. B., "A Partially Flux-Split Algorithm for Numerical Simulation of Compressible Inviscid and Viscous Flow," Proceedings of a Workshop on computational Fluid Dynamics, University of California, Davis, 1986.

8. Cummings, R. M., Rizk, Y. M., Schiff, L. B., and Chaderjian, N. M., "Navier-Stokes Predictions for the F-18 Wing and Fuselage at Large Incidence," *Journal of Aircraft*, Vol. 29, No. 4, 1992, pp. 565-574.

9. Rizk, Y. M. and Gee, K., "Unsteady Simulation of Viscous Flowfield Around F-18 Aircraft at Large Incidence," *Journal of Aircraft*, Vol. 29, No. 6, 1992, pp. 986-992.

10. Baldwin, B. and Lomax, H., "Thin-Layer Approximation and Algebraic Model for Separated Turbulent Flows," AIAA Paper 78-0257, January, 1978.

11. Degani, D. and Schiff, L. B., "Computation of Turbulent Supersonic Flows About Pointed Bodies Having Crossflow Separation," *Journal of Computational Physics*, Vol. 66, No. 1, 1986, pp. 183-196.

12. Ying, S. X., Schiff, L. B., and Steger, J. L., "A Numerical Study of Three-Dimensional Separated Flow Past a Hemisphere Cylinder," AIAA Paper 87-1207, June, 1987.

13. Benek, J. A., Steger, J. L., Dougherty, F. C., and Buning, P. G., "Chimera: A Grid Embedding Technique," AEDC-TR-85-64, Arnold Air Force Station, TN, 1986.

14. Erickson, G. E., "Wind Tunnel Investigation of Vortex Flows on F/A-18 Configuration at Subsonic Through Transonic Speeds," NASA Technical Paper 3111, December, 1991.

15. Gee, K., Rizk, Y. M., and Schiff, L. B., "Effect of Forebody Tangential Slot Blowing on flow About a Full Aircraft Geometry," AIAA Paper 93-2962, July, 1993.

Table 1. Jet exit conditions used in computational study.

16 inch slot starting 11 inches from the nose (16-11 in. slot)

M_∞	$\dot{m}$ (lb/sec)	MFR (x 10^{-3})	M_{jet}	P_{tot} (lb/in^2)	T_{tot} (°R)	P_e/P_a
0.243	0.056	0.015	0.125	5.65	402.	1.00
0.243	0.111	0.03	0.248	5.83	405.	1.00
0.243	0.224	0.06	0.50	6.63	420.	1.00
0.243	0.432	0.12	0.96	10.14	473.	1.00
0.243	0.668	0.18	1.00	15.76	480.	1.49
0.243	0.868	0.24	1.00	20.49	480.	1.94
0.400	0.187	0.03	0.43	6.15	415.	1.00
0.400	0.368	0.06	0.85	8.68	460.	1.00
0.400	0.714	0.12	1.00	16.84	480.	1.64
0.400	1.098	0.18	1.00	25.90	480.	2.53
0.400	1.427	0.24	1.00	33.68	480.	3.29
0.700	0.323	0.03	0.76	7.78	447.	1.00
0.700	0.639	0.06	1.00	15.10	480.	1.50
0.700	1.248	0.12	1.00	29.44	480.	2.93
0.700	1.871	0.18	1.00	44.17	480.	4.40
0.700	2.495	0.24	1.00	58.89	480.	5.86

24 inch slot starting 3 inches from the nose (24-3 in. slot)

M_∞	$\dot{m}$ (lb/sec)	MFR (x 10^{-3})	M_{jet}	P_{tot} (lb/in^2)	T_{tot} (°R)	P_e/P_a
0.243	0.056	0.015	0.081	5.62	401.	1.00
0.243	0.111	0.03	0.162	5.69	403.	1.00
0.243	0.224	0.06	0.325	6.04	409.	1.00
0.243	0.432	0.12	0.63	7.36	432.	1.00
0.243	0.668	0.18	0.96	10.21	475.	1.00
0.243	0.868	0.24	1.00	13.33	480.	1.26
0.400	0.187	0.03	0.28	5.71	407.	1.00
0.400	0.368	0.06	0.55	6.67	425.	1.00
0.400	0.714	0.12	1.00	10.97	480.	1.07
0.400	1.098	0.18	1.00	16.94	480.	1.66
0.400	1.427	0.24	1.00	21.94	480.	2.14
0.700	0.323	0.03	0.50	6.25	420.	1.00
0.700	0.639	0.06	1.00	9.86	480.	1.01
0.700	1.248	0.12	1.00	19.10	480.	1.92
0.700	1.871	0.18	1.00	28.75	480.	2.88
0.700	2.495	0.24	1.00	38.40	480.	3.85

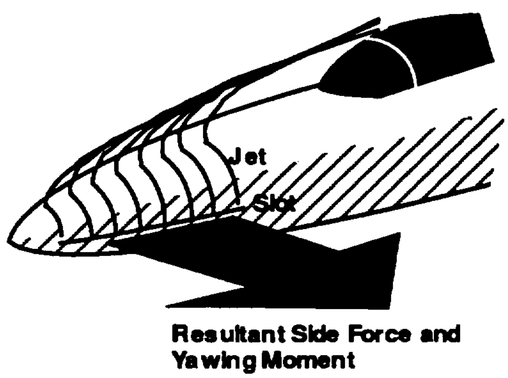

Fig. 1. Schematic of forebody tangential slot blowing concept.

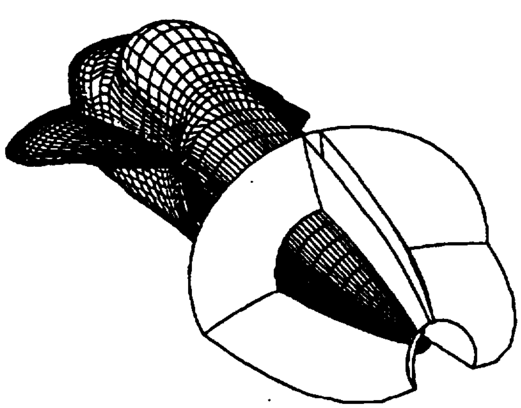

Fig. 2. Schematic of grid system used to model isolated F/A-18 forebody.

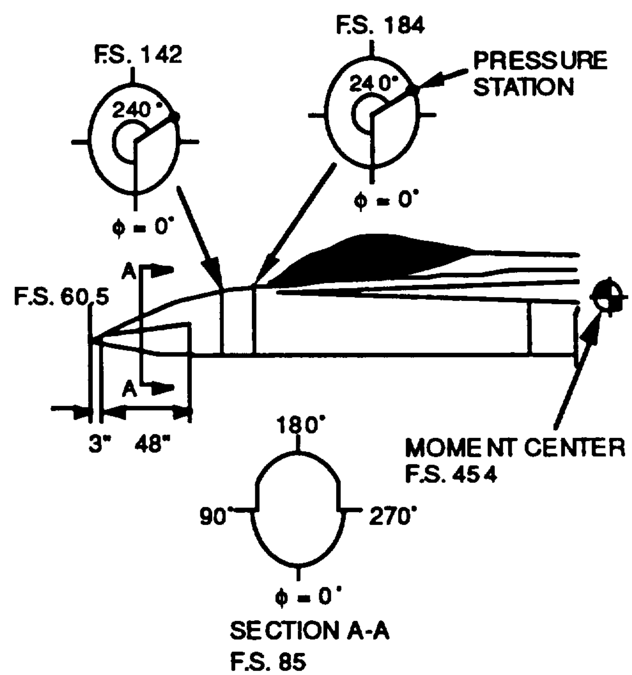

Fig. 3. Schematic of the slot configuration modeled in grid system.

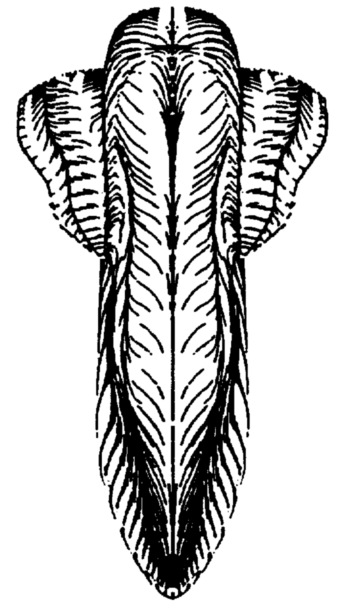

a) Surface flow pattern

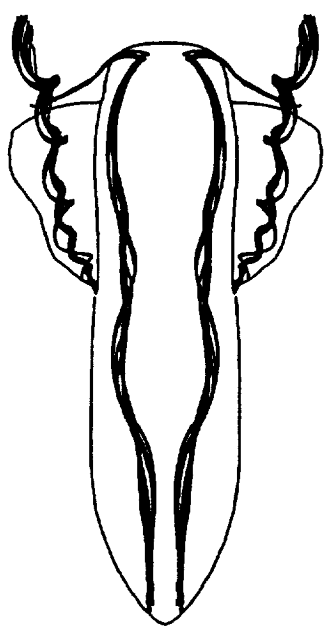

b)Off-surface instantaneous streamlines

Fig. 4. Flow field characteristics, M_∞ = 0.700, $\alpha = 30.3°$, $Re_{\bar{c}} = 31.4 \times 10^6$.

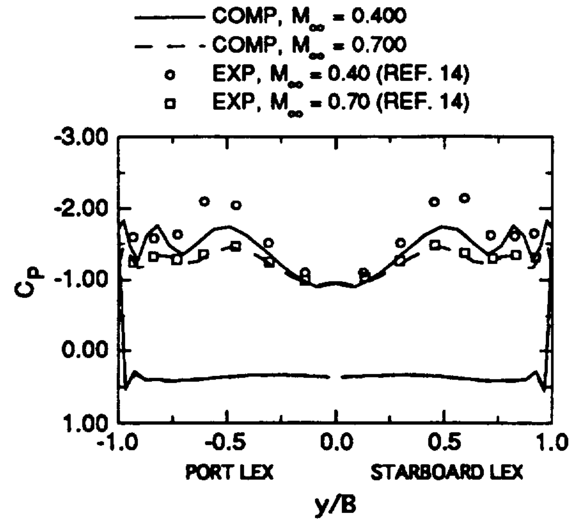

a) F. S. 253

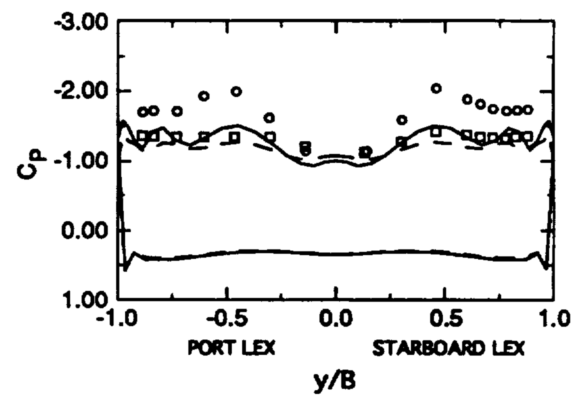

b) F. S. 296

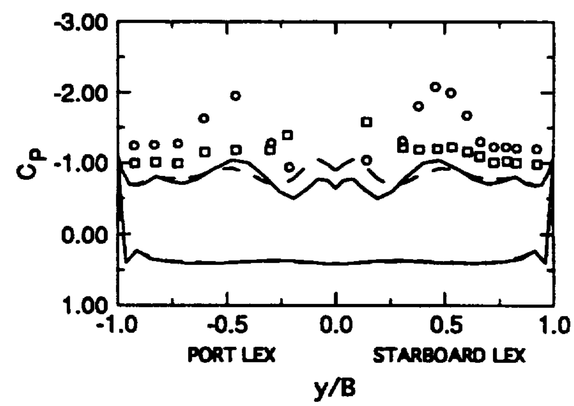

c) F. S. 357

Fig. 5. Comparison of computed surface pressure coefficient; $\alpha = 30.3°$.

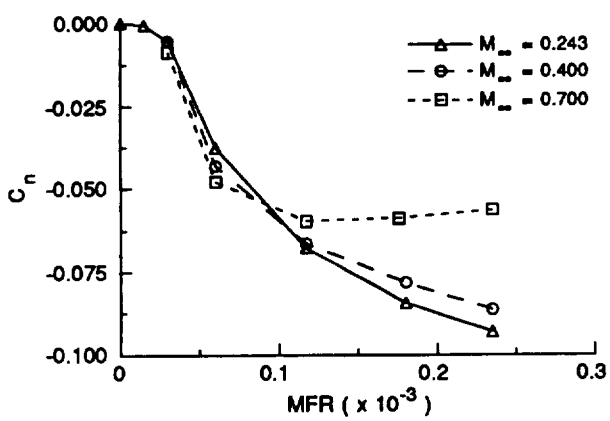

a) 16-11 in. slot

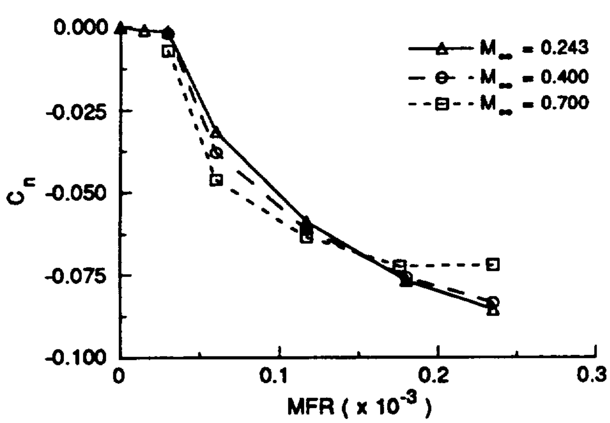

b) 24-3 in. slot

Fig. 6. Computed yawing moment plotted against MFR for isolated forebody with blowing; $\alpha = 30.3°$.

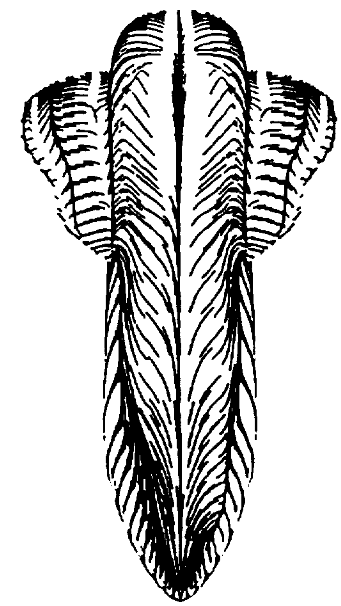

a) Surface flow pattern

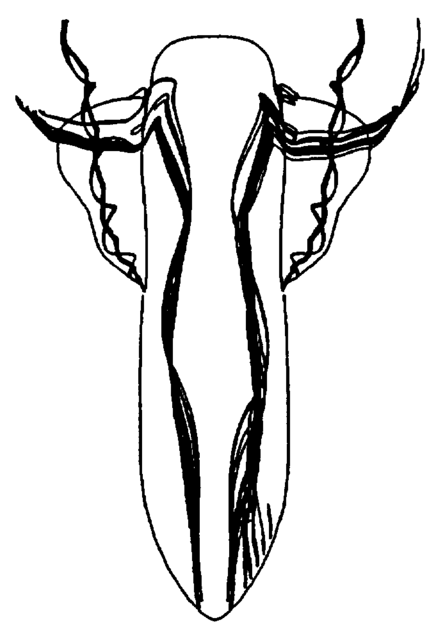

b)Off-surface instantaneous streamlines

Fig. 7. Flow field characteristics at low blowing rates. $M_\infty = 0.243$, $\alpha = 30.3°$, $Re_{\bar{c}} = 31.4 \times 10^{-6}$, MFR = 0.015×10^{-3}, 16-11 in. slot.

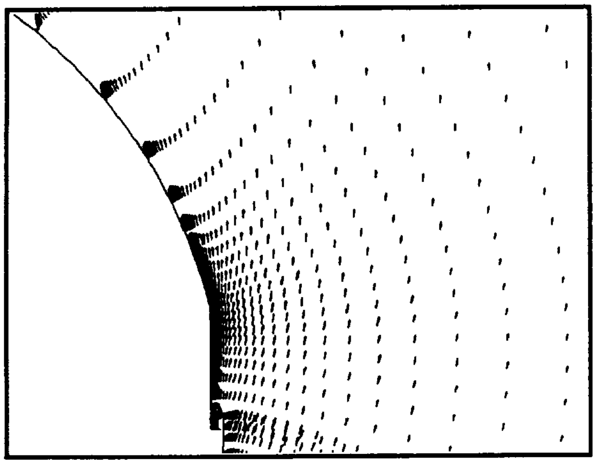

a) MFR = 0.06×10^{-3}, $P_e/P_a = 1.50$

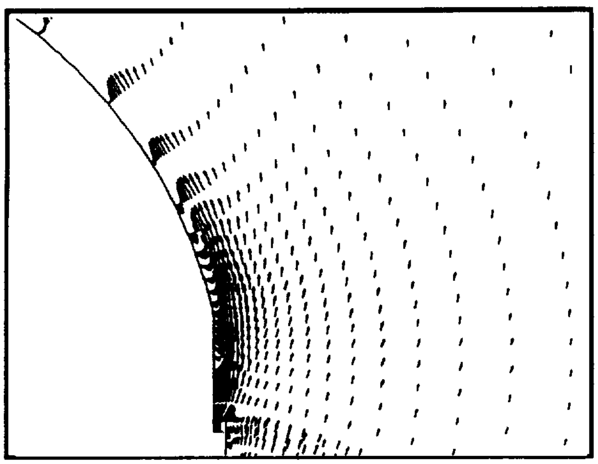

b) MFR = 0.24×10^{-3}, $P_e/P_a = 5.86$

Fig. 8. Effect of overblowing on flow in vicinity of the slot; computed velocity vectors in the crossflow plane at F.S. 75, $M_\infty = 0.700$, $\alpha = 30.3°$, $Re_{\bar{c}} = 31.4 \times 10^6$, 16-11 in. slot.

a) MFR = 0.06×10^{-3}, $P_e/P_a = 1.50$

b) MFR = 0.24×10^{-3}, $P_e/P_a = 5.86$

Fig. 9. Off-surface instantaneous streamlines with blowing. $M_\infty = 0.700$, $\alpha = 30.3°$, $Re_{\bar{c}} = 31.4 \times 10^6$, 16-11 in. slot.

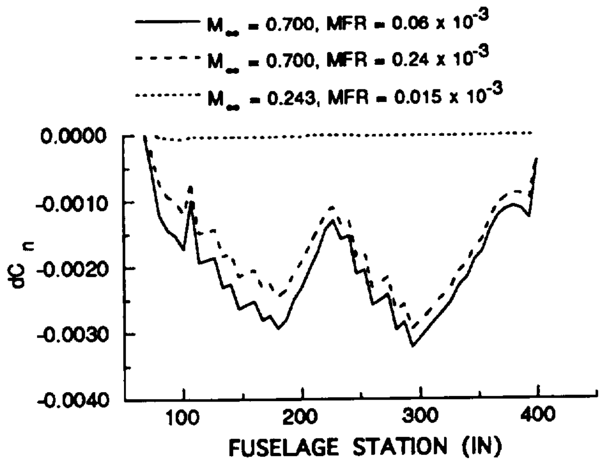

Fig. 10. Computed local yawing moment distribution with blowing, 16-11 in. slot.

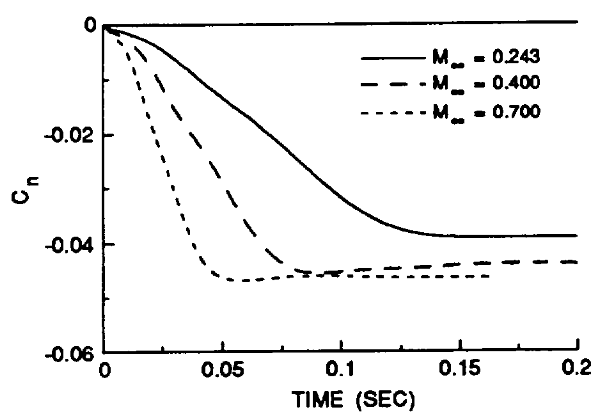

Fig. 11. Time history of forebody yawing moment. $M_\infty = 0.243$, $\alpha = 30.3°$, $Re_{\bar{c}} = 11.0 \times 10^6$, MFR = 0.06 x 10^{-3}, 16-11 in. slot.

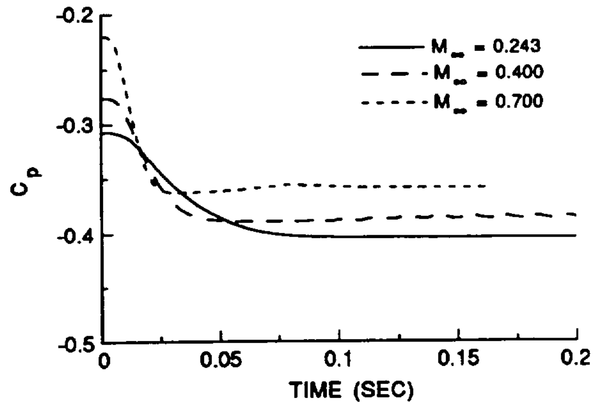

a) F. S. 142, $\phi = 240°$

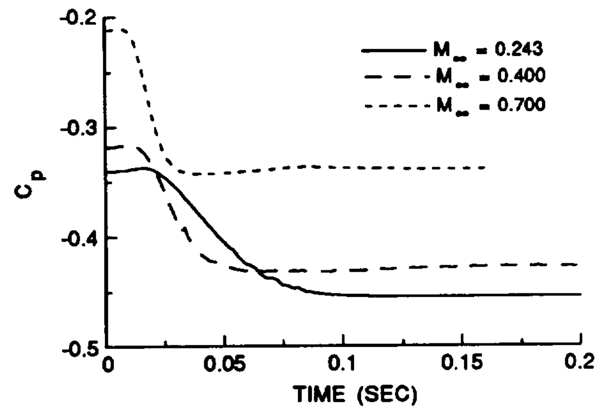

b) F. S. 184, $\phi = 240°$

Fig. 12. Time history of surface pressure coefficient. $M_\infty = 0.243$, $\alpha = 30.3°$, $Re_{\bar{c}} = 11.0 \times 10^6$, MFR = 0.06 x 10^{-3}, 16-11 in. slot.